EPJ Web of Conferences **71**, 00070 (2014)
DOI: 10.1051/epjconf/20147100070

Quenching of high-p_T hadrons: a non-energy-loss scenario

B. Z. Kopeliovich[1,a], J. Nemchik[2,3], I. K. Potashnikova[1], and Iván Schmidt[1]

[1] *Departamento de Física, Universidad Técnica Federico Santa María; Centro Científico-Tecnológico de Valparaíso, Avda. España 1680, Valparaíso, Chile*
[2] *Czech Technical University in Prague, FNSPE, Břehová 7, 11519 Prague, Czech Republic*
[3] *Institute of Experimental Physics SAS, Watsonova 47, 04001 Košice, Slovakia*

Abstract. A parton produced with a high transverse momentum in a hard collision is regenerating its color field, intensively radiating gluons and losing energy. This process cannot last long, if it ends up with production of a leading hadron carrying the main fraction z_h of the initial parton momentum. So energy conservation imposes severe constraints on the length scale of production of a single hadron with high p_T. As a result, the main reason for hadron quenching observed in heavy ion collision is not energy loss, but attenuation of the produced colorless dipole in the created dense medium. The latter mechanism, calculated with the path-integral methods, explains well the observed suppression of light hadrons and elliptic flow in a wide range of energies, from the lowest energy of RHIC up to LHC, and in a wide range of transverse momenta. The values of the transport coefficient extracted from data range within 1-2 GeV^2/fm, dependent on energy, so agree well with the theoretical expectations.

1 Intoduction

Single hadrons produced with high transverse momenta in heavy ion collisions at high energies of RHIC [1, 2] and LHC [3–5] turn out to be appreciably suppressed compared with pp collisions. While there is a consensus about the source of the suppression, which is final-state interaction with the co-moving medium, created in the collision, the mechanisms of the interaction is still under debate.

The popular interpretation of the observed suppression of high-p_T hadrons is the loss of energy by a parton propagating through the medium created in the collision. The perturbative radiative energy loss is caused by the "wiggling" of the parton trajectory due to multiple interactions in the medium. Every time, when the parton gets a kick from a scattering in the medium, a new portion of its color field is shaken off. The loss of energy induced by multiple interactions is naturally related to the broadening of the parton transverse (relative to its trajectory, i.e. to $\vec{p}_T$) momentum k_T [6],

$$\frac{dE}{dL} = -\frac{3\alpha_s}{4}\,\Delta k_T^2(L) = -\frac{3\alpha_s}{4}\int_0^L dl\,\hat{q}(l), \tag{1}$$

[a] e-mail: boris.kopeliovich@usm.cl

where $\hat{q}(l)$ is the rate of broadening Δk_T^2, which may vary with l along the parton trajectory,

$$\hat{q}(l) = \frac{d\Delta k_T^2}{dl}. \tag{2}$$

Although it is natural to expect that dissipation of energy by the parton in a medium should suppress production of leading hadrons, realization of this idea in detail raises many questions. In particular, one usually assumes that energy loss results in a shift in the argument of the fragmentation function, $z_h \Rightarrow z_H + \Delta z_h$. This could be true, if hadronization of the parton started outside the medium. However it starts right away after the hard collision, and the main part of gluon radiation occurs on a short distance (see section 2).

Another assumption, which the energy loss scenario relies upon and which has never been justified, is that the path length of the parton in the medium is always longer than the span of the medium. So the colorless hadronic state, which does not radiate energy any more and is eventually detected, is produced outside the medium. The validity of this assumption should be investigated and the path length available for hadronization should be evaluated. This problem was debated in [7] on a more certain situation of semi-inclusive deep-inelastic scattering, as well as within dynamical models of hadronization [8, 9] providing solid constraints on the above assumption.

Besides, theoretical arguments, some experimental data is also difficult to explain within the energy loss scenario. In particular, production of hadrons in semi-inclusive deeply inelastic scattering (SIDIS) offer a rigorous test for in-medium hadronization model in much more certain environment than in heavy ion collisions. Indeed in SIDIS off nuclei the medium density and geometry are well known and time independent; the fractional momentum z_h (the argument of the fragmentation function) of the detected hadron is measured. Measurements performed in the HERMES experiment [10, 11] well confirmed the predictions [12] made five years prior the measurements, within a model, which include evaluation of the hadronization length, which was found rather short. The comparison with data shown in Fig. 1 [7] demonstrate a good agreement.

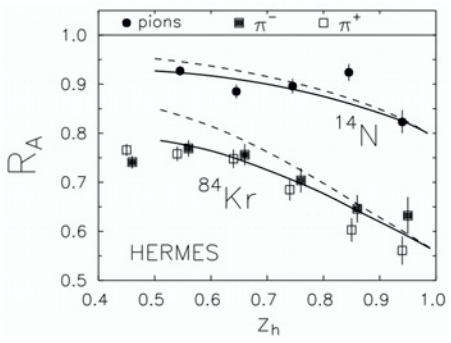

Figure 1. Comparison of the predicted [7, 12] z_h-dependence of the nuclear suppression factor in inclusive electroproduction of pions with HERMES data [10, 11]. Solid and dashed curves show the results with included or neglected energy loss corrections, respectively.

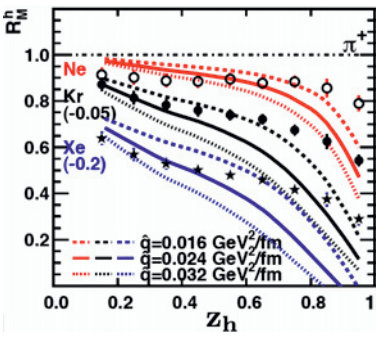

Figure 2. The results of description of the HERMES results by the model [13] based on the energy loss scenario, i.e. assuming a long time of hadronization. Several values of the transport coefficient are tested.

On the other hand the attempts to explain the same results of HERMES within the energy loss scenario were not successful. An example of comparison the model [13] with data [11] depicted in Fig. 2 show that the model fails to explain the data at large $z_h > 0.5$, which dominates high-p_T hadron production in heavy ion collision (see Fig. 5). Even adjustment of the transport coefficient $\hat{q}$ (actually well known for the cold nuclear matter [14, 15]) did not help.

Thus, the assumption of a long hadronization length should be checked thoroughly. The main space-time scales of the in-medium hadronization process are indicated schematically in Fig. 3. We

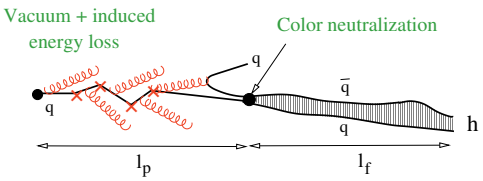

Figure 3. Space-time development of hadronization of a highly virtual quark producing a leading hadron carrying a substantial fraction z_h of the initial light-cone momentum.

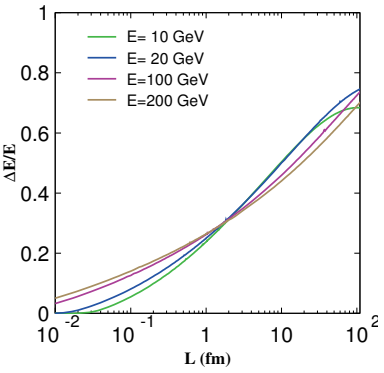

Figure 4. Fractional energy loss by a quark with different initial energies in vacuum vs path length L.

call production length l_p the distance at which color neutralization occurs and a colorless "pre-hadron" (a colorless state, which does not have any certain mass) is produced and starts developing a wave function. The latter process is characterized by the formation length, which usually is rather long, $l_f \sim 2E/(m_{h^*}^2 - m_h^2)$ [7, 17]. In what follows we concentrate on the production length scale l_p, which is the only path available for energy loss.

Notice that the question whether the hadronization ends up within or without the medium, might have no certain answer. This is a typical quantum-mechanical uncertainty: the production amplitudes with different values of l_p interfere. Such interference was evaluated in [18] for an example of a SIDIS process and found to be a considerable effect. However, an extension of those results to a hot medium is a challenge, so what follows we neglect the interference and employ the standard semi-classical space-time pattern of the production process.

2 Radiative energy loss in vacuum

First of all, one should discriminate between vacuum and medium-induced radiative energy loss. High-p_T partons radiate gluons and dissipate energy even in vacuum, and the corresponding rate of energy loss may considerably exceed the medium-induced value Eq. (1), because the former is caused by a hard collision.

2.1 Regeneration of the color field of a high-p_T parton

High-p_T scattering of partons leads to an intensive gluon radiation in forward-backward directions, which is related to the initial color field of the partons, shaken off due to the strong acceleration caused by the hard collision. The Weitzäcker-Williams gluons accompanying the colliding partons do not survive the hard interaction and lose coherence up to transverse frequencies $k \lesssim p_T$. Therefore, the produced high-p_T parton is lacking this part of the field and starts regenerating it via radiation of a new cone of gluons, which are aligned along the new direction. One can explicitly see the two cones of radiation in the Born approximation calculated in [19]. This process lasts a long time proportional to the jet energy ($E \approx p_T$), since the coherence length (or time) l_g of gluon radiation depends on the gluon fractional light-cone momentum x and its transverse momentum k relative to the jet axis as (to be concrete we assume that the jet is initiated by a quark),

$$l_g = \frac{2E}{M_{qg}^2 - m_q^2} = \frac{2Ex(1-x)}{k^2 + x^2 m_q^2}. \tag{3}$$

Here M_{qg} is the invariant mass of the recoil quark and radiated gluon.

One can trace how much energy is lost over the path length L via gluons which have lost coherence, i.e. were radiated, during this time interval,

$$\frac{\Delta E(L)}{E} = \int\limits_{\Lambda^2}^{Q^2} dk^2 \int\limits_0^1 dx\, x \frac{dn_g}{dx\, dk^2} \Theta(L - l_g), \tag{4}$$

where $Q \sim p_T$ is the initial quark virtuality; the infra-red cutoff is fixed at $\Lambda = 0.2$ GeV. The radiation spectrum reads

$$\frac{dn_g}{dx\, dk^2} = \frac{2\alpha_s(k^2)}{3\pi\, x} \frac{k^2[1 + (1-x)^2]}{[k^2 + x^2 m_q^2]^2} \tag{5}$$

A few examples of fractional vacuum energy loss by a quark vs distance from the hard collision is depicted in Fig. 4 for initial energies 10, 20, 100, 200 GeV (compare with heavy flavors in [20]). The rate of energy dissipation is considerable and energy conservation may become an issue for a long path length, if one wants to produce a leading hadron. Indeed, the production rate of high-p_T hadrons comes from a convolution of the the parton distributions in the colliding hadrons (which suppresses large fractional momenta x, i.e. high p_T), with the transverse momentum distribution in the hard parton collisions (also suppresses large p_T), and with the fragmentation function $D(z_h)$ of the produced parton. The latter has maximum at small $z_h \ll 1$, which, however, is strongly suppressed by the convolution, pushing the maximum towards large values of z_h. Numerical results of the convolution for the mean value $\langle z_h \rangle$ [21, 22] are depicted in Fig. 5, separately for quark and gluon jets (upper and bottom solid curves) and at different energies, $\sqrt{s} = 200,\ 2760$ and 7000 GeV. We see that the lower the collision energy is, the larger is $\langle z_h \rangle$, especially at high p_T, because the parton k_T distribution gets steeper. In the energy range of the LHC the magnitude of $\langle z_h \rangle$ practically saturates as function of $\sqrt{s}$ and p_T, and becomes indistinguishable for quark and gluonic jets.

It is worth emphasizing the difference between inclusive production of a high-p_T hadron and a high-p_T jet. In the former case, according to the above consideration, the detected hadron carries the main fractional light-cone momentum z_h of the jet, which it originates from. In the latter case, if only the whole jet transverse momentum p_T^{jet} is required to be large, and no other constraints are imposed, the fractional momenta of hadrons in the jet are typically very low, so energy conservation energy conservation does not imply any severe constraints on the hadronization time scale, which rises with p_T and may be long.

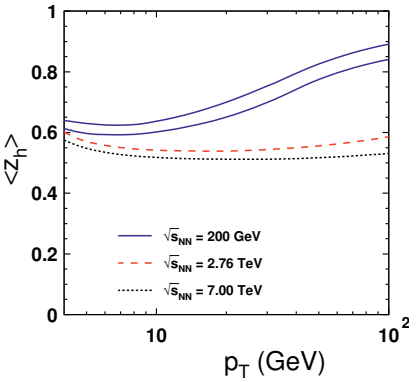

Figure 5. The mean fraction $\langle z_h \rangle$ of the jet energy carried by a hadron detected with transverse momentum p_T. The calculations are performed for collision energies $\sqrt{s} = 0.2,\ 2.76$ and 7 TeV.

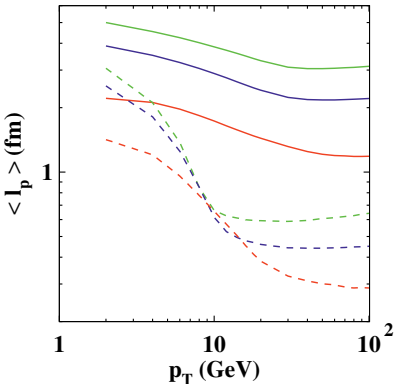

Figure 6. The mean production length as function of energy for quark (solid curves) and gluon (dashed curves) jets. In both cases the curves are calculated at $z_h = 0.5,\ 0.7,\ 0.9$ (from top to bottom).

2.2 How long does it take to produce a hadron?

Apparently, production of a hadron with fractional momentum z_h becomes impossible after the parton initiating the jet, radiates a substantial fraction of its initial energy, $\Delta E/E > 1 - z_h$. Thus, energy conservation imposes an upper bound for the production length l_p. Figures 4 and 5 show that such a maximal value of l_p is rather short. Remarkably, its value is nearly independent of p_T. This might seem to be in contradiction with the Lorentz factor, which should lead to $l_p \propto p_T$. However, the intensity of gluon radiation and the rate of energy loss also rise, approximately as p_T^2, what leads to an opposite effect of l_p reduction.

More precisely the p_T dependence of $\langle l_p \rangle$ can be derived within a dynamic model for hadronization. It was done in Ref. [9, 21] employing the model of perturbative hadronization [8]. Some numerical results are plotted in Fig. 6 for fragmentation of quarks and gluons by solid and dashed curves respectively. We see that the mean production length is rather short and slowly decreases with p_T. The production length for gluon jets is shorter, because of a more intensive vacuum energy loss and a stronger Sudakov suppression, which leads to a reduction of $\langle l_p \rangle$.

The production length in Fig. 6 demonstrates a trend to decrease with p_T, which is in variance with the naive expectation of a rise due to the Lorentz factor. As was explained above, this happens due to the growing virtuality and radiative dissipation of energy.

Notice that we took into consideration so far only the dissipation of energy in vacuum. Apparently, adding the medium induced energy loss one can only enhance the energy deficit and make the production length even shorter.

3 Propagation of color dipoles in a dense medium

As was discussed above, the intensive gluon radiation following the hard parton interaction, must stop in a short while (see Fig. 6) in order to be able to fragment into a hadron with large z_h (see Fig. 5) and to obey the energy conservation constraints. The gluon radiation can stop only by means of color neutralization and production of a colorless dipole. In vacuum (e.g. in pp collision) the matrix

element for a hadron production contains a direct projection of the initial distribution amplitude of the dipole separation to the hadron wave function,

$$A_{\rm vac} \propto \int_0^1 d\alpha \int d^2 r \, \Psi_h^\dagger(\vec{r},\alpha)\Psi_{in}(\vec{r},\alpha), \tag{6}$$

where Ψ_h and Ψ_{in} are the light-cone wave function of the hadron and the distribution amplitude of the produced dipole, respectively. We use the mixed representation of transverse dipole separation $\vec{r}$ and fractional light-cone momentum α carried by the quark.

In the case of production inside a medium, the produced dipole has to survive the propagation through the medium, i.e. to experience no inelastic collisions. The inelastic cross section depends on the dipole separation, which is fluctuating during the propagation. The effective way to solve this problem on a strict quantum-mechanical ground is the path integral method [17, 22]. In the case of in-medium production the matrix element Eq. (6) is modified to,

$$A_{\rm med} \propto \int_0^1 d\alpha \int d^2 r_1 d^2 r_2 \, \Psi_h^\dagger(\vec{r}_2,\alpha)\, G_{\bar{q}q}(l_1,\vec{r}_1;l_2,\vec{r}_2)\, \Psi_{in}(\vec{r}_1,\alpha). \tag{7}$$

Here $G_{\bar{q}q}(l_1,\vec{r}_1;l_2,\vec{r}_2)$ is the Green function describing propagation of the dipole between longitudinal coordinates l_1 and l_2 with initial and final separations $\vec{r}_1$ and $\vec{r}_2$ respectively. It satisfies the two-dimensional Schrödinger equation [23–26],

$$i\frac{d}{dl_2} G_{\bar{q}q}(l_1,\vec{r}_1;l_2,\vec{r}_2) = \left[\frac{m_q^2 - \Delta_{r_2}}{2\,p_T\,\alpha\,(1-\alpha)} - V_{\bar{q}q}(l_2,\vec{r}_2)\right] G_{\bar{q}q}(l_1,\vec{r}_1;l_2,\vec{r}_2) \tag{8}$$

The first term in square brackets plays role of kinetic energy in Schrödinger equation, while the imaginary part of the light-cone potential $V_{\bar{q}q}(l_2,\vec{r}_2)$ is responsible for absorption in the medium. The relation between the rate of broadening and the dipole cross section derived in [27], allows to present the imaginary part of the potential as [21, 28],

$$\mathrm{Im}\, V_{\bar{q}q}(l,\vec{r}) = -\frac{1}{4}\,\hat{q}(l)\, r^2. \tag{9}$$

Thus, color transparency [29] controls dipole attenuation in a medium.

The real part of the potential describes the nonperturbative interaction between q and $\bar{q}$ in the dipole [24, 30]. However, it should not affect much the dipole evolution on the initial perturbative stage of development. Therefore we will treat the $\bar{q}q$ as free noninteracting partons.

Measurements of the suppression of high-p_T hadrons in heavy ion collisions can provide precious information about the properties of the created hot matter. One can quantify those properties by the value of the transport coefficient $\hat{q}$, which is proportional to the medium density. The latter is time dependent, and is assumed to dilute as $\rho(t) = \rho_0\, t_0/t$ due to the longitudinal expansion of the produced medium. We adopt the popular parametrization [31] of the transport coefficient, which depends on impact parameter and path length (time) as,

$$\hat{q}(l,\vec{b},\vec{\tau}) = \frac{\hat{q}_0\, l_0}{l}\,\frac{n_{part}(\vec{b},\vec{\tau})}{n_{part}(0,0)}, \tag{10}$$

where $n_{part}(\vec{b},\vec{\tau})$ is the number of participants; $\hat{q}_0$ corresponds to the maximum medium density produced at impact parameter $\tau = 0$ in central collisions ($b = 0$) at the time $t = t_0 = l_0$ after the collision. In what follows we treat the transport coefficient $\hat{q}_0$ as an adjusted parameter.

4 Results at the energies of LHC

Now we are in a position to calculate the suppression factor $R_{AB}(b, p_T)$ for high-p_T hadrons produced in nuclear A-B collision with impact parameter b. The suppression orrurs due to the difference between the matrix elements (6) and (7), so we get,

$$R_{AB}(\vec{b}, p_T) = \frac{\int d^2\tau\, T_A(\tau) T_B(\vec{b}-\vec{\tau}) \int_0^{2\pi} \frac{d\phi}{2\pi} \left| \int_0^1 d\alpha \int d^2r_1 d^2r_2\, \Psi_h^\dagger(\vec{r}_2, \alpha) G_{\bar{q}q}(l_1, \vec{r}_1; l_2, \vec{r}_2) \Psi_{in}(\vec{r}_1, \alpha) \right|^2}{T_{AB}(b) \left| \int_0^1 d\alpha \int d^2r\, \Psi_h^\dagger(\vec{r}, \alpha) \Psi_{in}(\vec{r}, \alpha) \right|^2}. \quad (11)$$

where $T_{AB} = \int d^2\tau\, T_A(b) T_B(\vec{b}-\vec{\tau})$; ϕ is the azimuthal angle between the dipole trajectory and reaction plane (impact vector $\vec{b}$).

We also included medium-induced radiative energy loss during the short path from $l = l_0 \sim 1$ fm to $l = l_p$ (if $l_p > l_0$), where the parton experiences multiple interactions, which induce extra radiation of gluons and additional loss of energy [6],

$$\Delta E_{\rm med} = \frac{3\alpha_s}{4} \Theta(l_p - l_0) \int_{l_0}^{l_p} dl \int_{l_0}^{l} dl'\, \hat{q}(l'). \quad (12)$$

Although this is a small correction, it is included in the calculations by making a proper shift of the variable z_h in the fragmentation function.

The results of calculations [22] for charge hadron suppression factor $R_{AA}(p_T)$ are plotted in Fig. 7 in comparison with data from the ALICE [3] and CMS [4, 5] experiments at $\sqrt{s} = 2.76$ TeV and different centralities indicated in the plot. The dashed lines are calculated with the path-integral expression, Eq. (11), calculated with the space- and time dependent transport coefficient Eq. (10), where the parameter $\hat{q}_0 = 2\,\mathrm{GeV}^2/\mathrm{fm}$, which controls the normalization of R_{AA}, was adjusted to data. Notice that this parameter is independent of p_T and centrality. It affects the normalization, but not the shape of the p_T dependence. The solid curves also include the effects of initial state interactions (ISI) and energy conservation in nuclear collisions [32, 33], as is described below in Sect. 5.

As far as hadrons propagated over a longer path are suppressed more, naturally the azimuthal angle distribution of the produced hadrons correlates with the geometry of the collisions and gains an asymmetry. Data for such an asymmetry, characterized by the parameter $v_2 = \langle \cos(2\phi) \rangle$, provide an alternative sensitive way to test the model for suppression. The asymmetry can be calculated in a way similar to Eq. (11),

$$v_2(p_T, b) = \frac{\int d^2\tau\, T_A(\tau) T_B(\vec{b}-\vec{\tau}) \int_0^{2\pi} d\phi \cos(2\phi) \left| \int_0^\infty dr\, r\, \Psi_h(r) G_{\bar{q}q}(0, 0; \infty, r) \right|^2}{\int d^2\tau\, T_A(\tau) T_B(\vec{b}-\vec{\tau}) \int_0^{2\pi} d\phi \left| \int_0^\infty dr\, r\, \Psi_h(r)\, G_{\bar{q}q}(0, 0; \infty, r) \right|^2}. \quad (13)$$

Here we neglected the initial dipole size $r_1 \sim 1/p_T \approx 0$ at $l_1 = 0$. The results of calculations [22] are compared in Fig. 8 with data from the ALICE [34] and CMS [35] experiments at $\sqrt{s} = 2.76$ TeV and different centralities. The calculated asymmetry in the perturbative regime is rather small and is falling monotonically with p_T in agreement with data.

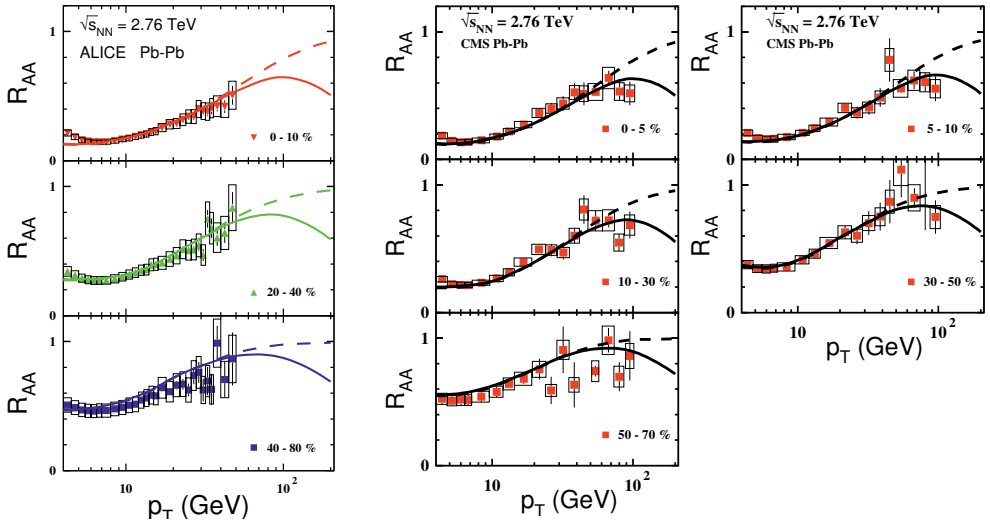

Figure 7. Centrality dependence of the suppression factor $R_{AA}(p_T, b)$ measured in the ALICE [3] (*left*) and CMS [4, 5] (*right*) experiments at $\sqrt{s} = 2.76\,\text{TeV}$. The intervals of centrality are indicated. The dashed lines are calculated with Eq. (11). The solid curves also include the effects of initial state interactions [32, 33], as is described in Sect. 5.

Notice that an azimuthal asymmetry appears for any mechanism of suppression. One may wonder if a successful description of the cross section (Fig. 7) should automatically lead to a good agreement with $v_2(p_T)$, i.e. whether data for v_2 suggest a complementary test of the model? The answer is positive, v_2 data provide a more stringent examination of the model. Indeed, while the suppression of the cross section depends on the accumulated suppression along the hadron path in the medium, azimuthal asymmetry is sensitive to the path length distribution.

5 Large x_T, towards the kinematic bound

Multiple interactions of the projectile hadron and its debris propagating through the nucleus lead to a dissipation of energy. Important observation made in [32] (see also [36]) is that the resulting loss of energy is proportional to the energy of the projectile hadron, therefore the related effects do not disappear at very high energies. An easy and intuitive way to understand this is the Fock state representation for the projectile hadron wave function. Those sates are the fluctuations of this hadron "frozen" by Lorentz time dilation. The interaction with the target modifies the weights of the Fock states, some interact stronger, some weaker. An example is the light-cone wave function of a transversely polarized photon [37]. In vacuum it is overwhelmed by $\bar{q}q$ Fock states with vanishingly small separation (this is why the normalization of the wave function is ultraviolet divergent). However, those small size fluctuations have a vanishingly small interaction cross section, and the photoabsorption cross section turns out to be finite.

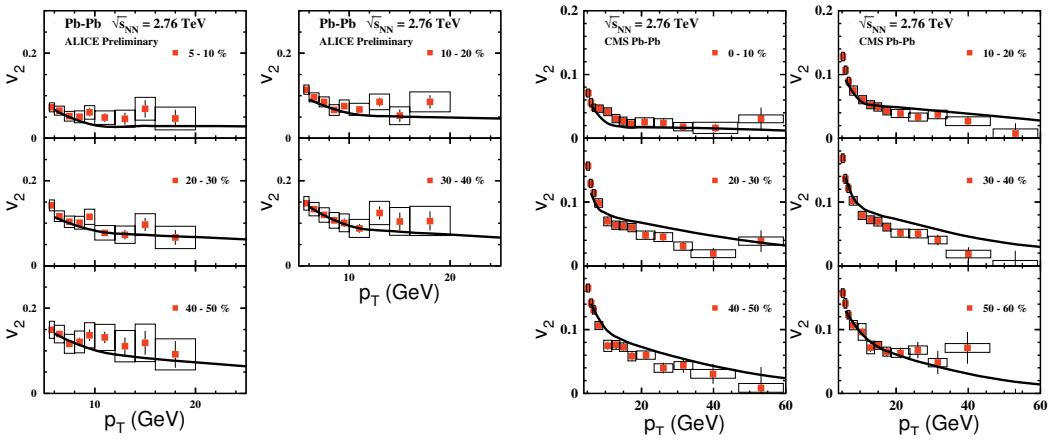

Figure 8. Data from the ALICE [34] (*left*) and CMS [35] (*right*) experiments for azimuthal anisotropy, $v_2(p_T)$ in lead-lead collisions at $\sqrt{s} = 2.76$ TeV and different centralities. The curves present the results of calculation with Eq. (13).

In each Fock component the hadron momentum is shared by the constituents, and the momentum distribution depends on their multiplicity: the more constituents the Fock state contains, the smaller is the mean fractional momentum per a constituent parton. Higher Fock components interact with a nuclear target stronger and gain larger weight factors compared to low Fock states. Thus, the x distribution in the projectile hadron is softer on a nuclear than on a proton targets.

In the case of a hard reaction on a nucleus, such softening of the momentum distribution of a projectile parton can be viewed as an effective loss of energy of the leading parton due to initial state multiple interactions: the mean energy of the leading parton on a nuclear target decreases compared the hard reaction on a proton target. Such a reduction of the fractional momentum of the leading parton is apparently independent of the initial hadron energy. Thus, the effective loss of energy is proportional to the initial energy.

Notice that this is different from energy loss by a single parton propagating through a medium and experiencing induced gluon radiation. In this case the mean fractional energy carried the radiated gluons vanishes at large initial energies E as $\Delta E/E \propto 1/E$ [6, 38, 39].

Initial state energy loss is a minor effect at high energies and mid rapidities. However, it may essentially suppress the cross section upon approaching the kinematic bound, either $x_L = 2p_L/\sqrt{s} \to 1$ or $x_T = 2p_T/\sqrt{s} \to 1$. Correspondingly, the proper variable, which controls this effect is $\xi = \sqrt{x_L^2 + x_T^2}$. The magnitude of suppression was evaluated in [32, 33]. It was found that each of multiple interactions (treated within the Glauber approximation) in the nucleus supplies a suppression factor $U(\xi) \approx 1 - \xi$. Summing up over the multiple ISI interactions in pA collision with impact parameter b one arrives at a new parton distribution function in the projectile proton compared with pp collisions,

$$F_{i/p}^{(A)}(x, Q^2, b) = C\, F_{i/p}(x, Q^2)\, \frac{\left[e^{-\xi\sigma_{eff}T_A(b)} - e^{-\sigma_{eff}T_A(b)}\right]}{(1-\xi)\left[1 - e^{-\sigma_{eff}T_A(b)}\right]}. \tag{14}$$

Here σ_{eff} is the effective hadronic cross section controlling multiple interactions. It is reduced by Gribov inelastic shadowing, which makes the nuclear medium more transparent. The effective cross section was evaluated in [32, 40] at about $\sigma_{eff} \approx 20\,\mathrm{mb}$. The normalization factor C in Eq. (14) is fixed by the Gottfried sum rule.

With the parton distribution functions Eq. (14) modified by ISI energy loss one achieves a good parameter-free description of available data from the BRAHMAS [41] and STAR [42] experiments at forward rapidities in dA collisions large x_L [32, 33].

The ISI energy-loss should also be important at large p_T, in particular in the RHIC energy range, where x_T in data reaches values of $0.2 - 0.3$. Notice that the real values of x_T, essential for energy conservation, are about twice larger, $\tilde{x}_T = x_T/z_h$, so it reaches values of 0.5 at RHIC, and about 0.4 at LHC. The measured nuclear modification of pions produced at high p_T in dAu collisions at $\sqrt{s} = 200\,\mathrm{GeV}$ [43] indeed demonstrates a significant suppression, as one can see in Fig. 9. With the same modification factor Eq. (14), which was successful at forward rapidities, a good agreement is achieved at large p_T as well, as is demonstrated in Fig. 9.

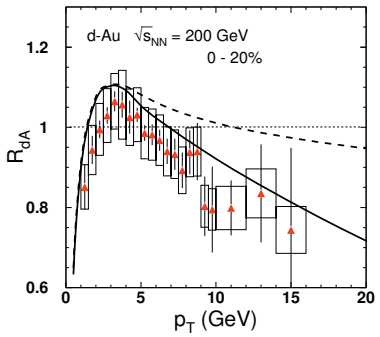

Figure 9. Nuclear attenuation factor $R_{dAu}(p_T)$ for π^0 mesons produced in central $(0-20\%)$ d-Au collisions at $\sqrt{s} = 200\,\mathrm{GeV}$ and $\eta = 0$. The solid and dashed curves show the predictions calculated with and without the ISI corrections. Isotopic effect is included. The data are from the PHENIX experiment [43].

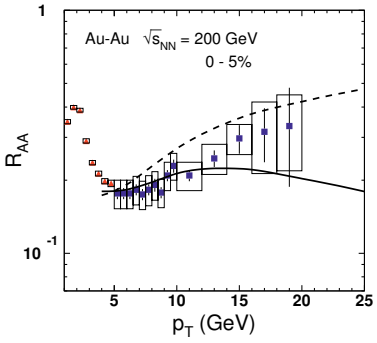

Figure 10. Nuclear attenuation factor $R_{AA}(p_T)$ for neutral pions produced in central gold-gold collisions at $\sqrt{s} = 200$ GeV. The solid and dashed lines are calculated with or without ISI corrections. PHENIX data are from [44] (triangles) and [45] (squares).

The effects of ISI energy loss also affect the p_T dependence of the nuclear suppression in heavy ion collisions. These effects are calculated similarly, using the modified parton distribution functions Eq. (14) for nucleons in both colliding nuclei. The resulting additional suppression significantly reduces $R_{AA}(p_T)$ at the energy of RHIC. This is demonstrated in Fig. 10 on the example of central gold-gold collisions at $\sqrt{s} = 200\,\mathrm{GeV}$. Since parameter q_0 is expected to vary with energy, it was readjusted and found to be $q_0(RHIC) = 1.6\,\mathrm{GeV}^2/\mathrm{fm}$, less than in collisions at the LHC[1]. Data on centrality dependence of $R_{AA}(p_T)$, presented in Fig. 10, is also well explained.

One can access larger values of x_T either by increasing p_T and a fixed energy, or by reducing the collision energy keeping unchanged the p_T range. So the data [46] at lower energies $\sqrt{s} = 62\,\mathrm{GeV}$ depicted in Fig. 11 play important role for study of the energy loss effects. Indeed, the data demonstrate an unusual falling p_T dependence of $R_{AA}(p_T)$ predicted with the suppression factor Eq. (14).

[1] Notice that q_0 is also A-dependent.

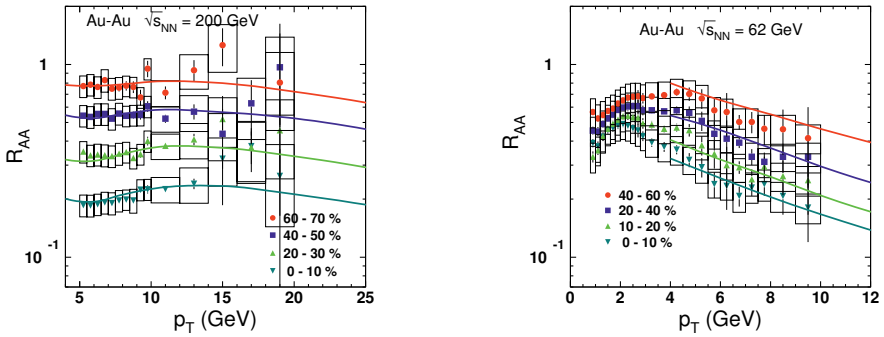

Figure 11. Centrality dependence of the suppression factor $R_{AA}(p_T, b)$ measured in the PHENIX experiment in gold-gold collisions at $\sqrt{s} = 200\,\text{GeV}$ [44](*left*) and $\sqrt{s} = 62\,\text{GeV}$ [46] (*right*). The intervals of centrality are indicated in the plot.

On the contrary, at much higher energies of LHC one would not expect any sizable effects of energy loss. Nevertheless, even at such high energies one can reach x_T sufficiently large for ISI energy loss effects to show up. The results depicted by solid curves in Fig. 7 include such energy loss corrections, which cause leveling off and even fall of $R_{AA}(p_T)$ at $p_T \gtrsim 100\,\text{GeV}$.

6 Summary

Summarizing, for the process of inclusive high-p_T hadron production we performed evaluation of the production length l_p available for gluon radiation and energy loss, and found it to be rather short in many instances. As a result, the main reason for the observed suppression in heavy ion collisions is not induced energy loss, but attenuation of early produced color dipoles propagating through a dense absorptive matter. Having no free parameters, except the medium density characterized by the transport coefficient $\hat{q}$, we reached a good agreement with data on nuclear suppression and azimuthal elliptic flow in a wide range of energy, from the lowest energies of RHIC up to LHC, and in a wide range of transverse momenta, from $p_T = 5$-$7\,\text{GeV}$ up to $100\,\text{GeV}$. The region of smaller p_T apparently is dominated by hydrodynamic mechanisms of hadron production. The recent attempt [50] to unify hydrodynamics with perturbative QCD calculations, presented above, was successful, the whole range of $p - T$ was well described with the same medium temperature.

Our analysis led to quite reasonable values of the parameter characterizing the hot medium, $q_0 = 1.2,\ 1.6$ and $2\,\text{GeV}^2/\text{fm}$ at $\sqrt{s} = 62,\ 200$ and $2760\,\text{GeV}$ respectively. This is close to the expected magnitude $q_0 \sim 1\,\text{GeV}^2/\text{fm}$ [6], as well as to the value extracted from data on J/Ψ suppression [28, 47]. The latter is an alternative probe for the created hot matter, and different probes obviously must result in the same properties of the probed medium. The pure energy loss scenario did not pass this important test, it leads to a magnitude of the transport coefficient [48], which is an order of magnitude larger than expected [6].

Another important test of the energy loss scenario would be a direct measurement of the transport coefficient, i.e. broadening of a jet propagating through the hot medium. On the contrary to this expectation no broadening was found in back-to-back photon-jet azimuthal correlation [49].

Concluding, few words of precotion to avoid further confusions:

(i) One should clearly distinguish between vacuum and medium-induced radiative energy loss. The former is much more intensive and is the main reason for shortness of l_p.

(ii) One should also discriminate between the terms "jet quenching" and "hadron quenching". The latter is what was considered in this paper, a hadron detected inclusively with a high p_T carries the main fraction z_h of the accompanying jet. This is why intensive vacuum energy loss and energy conservation impose severe constraints on the value of l_p. If, however, the whole jet has a large p_T, while none of hadrons in the jet are not forced to have large z_h, the hadronization length is subject to the usual Lorentz time dilation and is long.

Acknowledgments: This work was supported in part by Fondecyt (Chile) grants 1130543, 1130549, 1100287, and by Conicyt-DFG grant No. RE 3513/1-1. The work of J.N. was partially supported by the grant 13-02841S of the Czech Science Foundation (GAČR), by the Grant VZ MŠMT 6840770039, by the Slovak Research and Development Agency APVV-0050-11 and by the Slovak Funding Agency, Grant 2/0092/10.

References

[1] S. S. Adler *et al.* [PHENIX Collaboration], Phys. Rev. Lett. **91**, 072301 (2003).
[2] J. Adams *et al.* [STAR Collaboration], Phys. Rev. Lett. **91**, 072304 (2003).
[3] B. Abelev *et al.* [ALICE Collaboration], Phys. Lett. B **720**, 52 (2013).
[4] Y.-J. Lee (for the CMS Collaboration), J. Phys. G **38**, 124015 (2011).
[5] A. S. Yoon (for the CMS Collaboration), J. Phys. G **38**, 124116 (2011).
[6] R. Baier, Y. L. Dokshitzer, S. Peigne and D. Schiff, Phys. Lett. B **345**, 277 (1995); Nucl. Phys. B **484**, 265 (1997).
[7] B. Z. Kopeliovich, J. Nemchik, E. Predazzi and A. Hayashigaki, Nucl. Phys. A **740**, 211 (2004).
[8] B. Z. Kopeliovich, H. -J. Pirner, I. K. Potashnikova, I. Schmidt and A. V. Tarasov, Phys. Rev. D **77**, 054004 (2008).
[9] B. Z. Kopeliovich, H. -J. Pirner, I. K. Potashnikova and I. Schmidt, Phys. Lett. B **662**, 117 (2008).
[10] A. Airapetian *et al.* [HERMES Collaboration], Eur. Phys. J. C **20**, 479 (2001).
[11] A. Airapetian *et al.* [HERMES Collaboration], Phys. Lett. B **577**, 37 (2003).
[12] B. Z. Kopeliovich, J. Nemchik and E. Predazzi, Proceedings of the workshop on Future Physics at HERA, ed. by G. Ingelman, A. De Roeck and R. Klanner, DESY 1995/1996, v.2, 1038 (1996) [nucl-th/9607036]; Proceedings of the ELFE Summer School on Confinement Physics, ed. by S. D. Bass, P. A. M. Guichon, Editions Frontieres, Cambridge, 391, (1995) [hep-ph/9511214].
[13] W. T. Deng and X. N. Wang, Phys. Rev. C **81**, 024902 (2010).
[14] B. Z. Kopeliovich, I. K. Potashnikova and I. Schmidt, Phys. Rev. C **81**, 035204 (2010).
[15] S. Domdey, D. Grunewald, B. Z. Kopeliovich and H. J. Pirner, Nucl. Phys. A **825**, 200 (2009).
[16] B. Z. Kopeliovich, H. -J. Pirner, I. K. Potashnikova, I. Schmidt, A. V. Tarasov and O. O. Voskresenskaya, Phys. Rev. C **78**, 055204 (2008).
[17] B. Z. Kopeliovich and B. G. Zakharov, Phys. Rev. D **44**, 3466 (1991).
[18] B. Z. Kopeliovich, H. -J. Pirner, I. K. Potashnikova, I. Schmidt, A. V. Tarasov and O. O. Voskresenskaya, Phys. Rev. C **78**, 055204 (2008).
[19] J. F. Gunion and G. Bertsch, Phys. Rev. D **25**, 746 (1982).
[20] B. Z. Kopeliovich, I. K. Potashnikova and I. Schmidt, Phys. Rev. C **82**, 037901 (2010).
[21] B. Z. Kopeliovich, I. K. Potashnikova and I. Schmidt, Phys. Rev. C **83**, 021901 (2011).

[22] B. Z. Kopeliovich, J. Nemchik, I. K. Potashnikova and I. Schmidt, Phys. Rev. C **86**, 054904 (2012).
[23] B. Z. Kopeliovich, A. V. Tarasov and A. Schäfer, Phys. Rev. C **59**, 1609 (1999).
[24] B.Z. Kopeliovich, A. Schäfer and A.V. Tarasov, Phys. Rev. D **62**, 054022 (2000).
[25] B. Z. Kopeliovich, J. Raufeisen and A. V. Tarasov, Phys. Lett. B **440**, 151 (1998).
[26] B. G. Zakharov, Phys. Atom. Nucl. **61**, 838 (1998) [Yad. Fiz. **61**, 924 (1998)]
[27] M. B. Johnson, B. Z. Kopeliovich and A. V. Tarasov, Phys. Rev. C **63**, 035203 (2001).
[28] B. Z. Kopeliovich, I. K. Potashnikova and I. Schmidt, Phys. Rev. C **82**, 024901 (2010).
[29] B. Z. Kopeliovich, L. I. Lapidus and A. B. Zamolodchikov, JETP Lett. **33**, 595 (1981) [Pisma Zh. Eksp. Teor. Fiz. **33**, 612 (1981)].
[30] B. Z. Kopeliovich, J. Nemchik, A. Schäfer and A. V. Tarasov, Phys. Rev. C **65**, 035201 (2002).
[31] X. F. Chen, C. Greiner, E. Wang, X. N. Wang and Z. Xu, Phys. Rev. C **81**, 064908 (2010).
[32] B. Z. Kopeliovich, J. Nemchik, I. K. Potashnikova, M. B. Johnson and I. Schmidt, Phys. Rev. C **72**, 054606 (2005).
[33] B. Z. Kopeliovich and J. Nemchik, J. Phys. G G **38**, 043101 (2011).
[34] A. Dobrin (for the ALICE Collaboration), J. Phys. G **38**, 124170 (2011).
[35] S. Chatrchyan *et al.* [CMS Collaboration], Phys. Rev. Lett. **109**, 022301 (2012).
[36] F. Arleo, S. Peigne and T. Sami, Phys. Rev. D **83**, 114036 (2011).
[37] B. Z. Kopeliovich, J. Raufeisen and A. V. Tarasov, Phys. Rev. C **62**, 035204 (2000).
[38] F. Niedermayer, Phys. Rev. D **34**, 3494 (1986).
[39] S.J. Brodsky and P. Hoyer, Phys. Lett. B **298**, 165 (1993).
[40] B. Z. Kopeliovich, I. K. Potashnikova and I. Schmidt, Phys. Rev. C **73**, 034901 (2006).
[41] I. Arsene, et al. [BRAHMS Collaboration] Phys. Rev. Lett. **93**, 242303 (2004).
[42] J. Adams et al. [STAR Collaboration] Phys. Rev. Lett. **97**, 152302 (2006).
[43] S. S. Adler *et al* [PHENIX Collaboration] 2007 Phys. Rev. Lett. **98**, 172302 (2007).
[44] A. Adare *et al.* [PHENIX Collaboration], Phys. Rev. C **87**, 034911 (2013).
[45] M. L. Purschke (for the PHENIX Collaboration), J. Phys. G **38**, 124016 (2011).
[46] PHENIX Collaboration, preliminary data posted at www.phenix.bnl.gov/WWW/plots/show_plot.php?editkey=p1118
[47] B. Z. Kopeliovich, Nucl. Phys. A **854**, 187 (2011).
[48] A. Adare *et al.* [PHENIX Collaboration], Phys. Rev. C **77**, 064907 (2008).
[49] S. Chatrchyan *et al.* [CMS Collaboration], Phys. Lett. B **712**, 176 (2012).
[50] J. Nemchik, I. . A. Karpenko, B. Z. Kopeliovich, I. K. Potashnikova and Y. . M. Sinyukov, arXiv:1310.3455 [hep-ph].